

FORECAST SOLAR IRRADIANCE USING ARTIFICIAL NEURAL NETWORKS VIA ASSESSMENT OF ROOT MEAN SQUARE ERROR

DỰ BÁO BỨC XẠ MẶT TRỜI SỬ DỤNG MẠNG NƠ-RON NHÂN TẠO
THÔNG QUA ĐÁNH GIÁ SAI SỐ BÌNH PHƯƠNG TRUNG BÌNH

Nguyen Duc Tuyen^{1,*},
Vu Xuan Son Huu¹, Nguyen Quang Thuan²

ABSTRACT

Forecasting solar irradiance has been an important topic and a trend in renewable energy supply share. Exact irradiance forecasting could help facilitate the solar power output prediction. Forecasting improves the planning and operation of the Photovoltaic (PV) system and the power system, then yields many economic advantages. The irradiance can be forecasted using many methods with their accuracies. This paper suggests two methods based on AI which approach forecasting solar irradiance by getting data from solar energy resources and Meteorological data on the Internet as inputs to an Artificial Neural Network (ANN) model. Since the inputs involved are the same as the ones available from a recently validated forecasting model, there are root mean square error (RMSE) and mean absolute error (MAE) comparisons between the established forecasting models and the proposed ones.

Keywords: Solar Irradiance Forecasting; Artificial Neural Network; RMSE.

TÓM TẮT

Dự báo bức xạ mặt trời đã dần trở thành một chủ đề quan trọng và một xu hướng trong việc phát triển các nguồn năng lượng tái tạo. Dự báo bức xạ chính xác sẽ giúp dự báo công suất phát điện mặt trời. Dự báo hỗ trợ cho việc lập kế hoạch và vận hành hệ thống điện mặt trời nói riêng và hệ thống điện nói chung, từ đó đem lại nhiều lợi ích kinh tế. Bức xạ có thể được dự đoán bằng nhiều phương pháp khác nhau với độ chính xác khác nhau. Bài báo này đề cập đến hai phương pháp dự đoán bức xạ mặt trời dựa trên việc sử dụng trí tuệ nhân tạo, qua đó để xuất các mô hình dự báo bức xạ mặt trời ngắn hạn thông qua dữ liệu năng lượng mặt trời và khí tượng trên Internet làm đầu vào cho mô hình mạng nơ-ron nhân tạo. Khi các đầu vào giống như các biến từ một mô hình dự báo được kiểm chứng, chúng ta có sự so sánh sai số bình phương trung bình (RMSE) và sai số tuyệt đối trung bình (MAE) giữa mô hình được xây dựng và mô hình đã đề xuất.

Từ khóa: Dự báo bức xạ mặt trời; mạng nơ-ron nhân tạo; RMSE.

NOMENCLATURE

RNN	Recurrent Neural Network
LSTM	Long Short Term Memory
MAE	Mean Absolute Error
BPTT	Backpropagation Through Time
RMSE	Root Mean Square Error

1. INTRODUCTION

The increase in fossil fuel prices and the decrease of Photovoltaic (PV) panel production cost have spurred the integration of renewable energy sources. Renewable energy sources have many advantages, including being environment-friendly and sustainable. However, these sources are highly intermittent. That is, the output power of renewable sources is variable and can be considered as a varying non-stationary time series. Solar PV systems are one of the main renewable energy sources. The output of PV is highly dependent on solar irradiance, temperature, and different weather parameters. Predicting solar irradiance means that the output of PV is predicted one or more steps ahead of time. The solar irradiance prediction can lead to an improvement in the power quality of electric power delivered to the consumers [1]. It can also lead to more efficient energy management in the smart grid [2]. One of the approaches used for solar power prediction involves the use of artificial neural networks (ANNs). Many methodologies have been developed over the years which are based on ANNs.

Using a backpropagation (BP) neural network, the solar radiation data from the past 24-h was used to predict the value for the next instance in [3]. The mean daily solar radiation data and air temperature values were used to predict future values up to 24-h and ANN was implemented in [4]. The reference [5] is proposed on estimating accurate values of solar global irradiation (SGI) on tilted planes via

¹School of Electrical Engineering, Hanoi University of Science and Technology

²Hanoi University of Industry

*Email: tuyen.nguyenduc@hust.edu.vn

Received: 20/01/2020

Revised: 16/6/2020

Accepted: 23/12/2020

ANN. The recurrent neural network has also been proposed for the prediction of solar energy. Elman neural networks were compared with an adaptive neuro-fuzzy inference system (ANFIS), multi-layer perceptron (MLP) and neural network autoregressive model with an exogenous model (NNARX) in [6]. The simulation of Deep recurrent neural networks (DRNNs) method for forecasting solar irradiance will be compared to several common methods such as support vector regression and feedforward neural networks (FNN) [7].

In this paper, two methods for forecasting solar irradiance (Recurrent Neural Network and Long Short-Term Memory) are discussed comprehensively. A performance comparison of each proposed method with established forecasting models is presented by assessing Root Mean Square Error (RMSE) and Mean Absolute error (MAE). After that, the advantages and disadvantages of these methods are indicated thus the improvements for each instance are shown.

2. METHODS

2.1. Recurrent Neural network (RNN)

A recurrent neural network is a type of neural network used in modeling and prediction of sequential data where the output is dependent on the input [7]. For tasks that involve sequential inputs, such as speech and language, it is often better to use RNN. RNNs process an input sequence one element at a time, maintaining in their hidden units a 'state vector' that implicitly contains information about the history of all the past elements of the sequence. Therefore, the RNN is capable of predicting a random sequence of inputs thanks to its internal memory. The internal memory can store information about previous calculations. Fig. 1 shows the basic RNN, where the hidden neuron h has feedback from other neurons in an earlier time step multiplied by a weight W . When basic RNN is spread out into a full network, it can be seen that the input of a hidden neuron takes an input from neurons at the previous time step [8].

The input x_t at instant time t is multiplied by the input weight vector to obtain the input of the first hidden neuron. Then, the next hidden neuron, h_{t+1} , will have the input of x_{t+1} and the previously hidden neuron h_t multiplied by the weight W of the hidden neuron. The output neurons take the input only from the hidden neurons multiplied by the output weight V . RNNs are very powerful dynamic systems:

$$h_t = g_h(U \times x_t + W \times h_{t-1}) \quad (1)$$

$$y_t = g_y(V \times h_t) \quad (2)$$

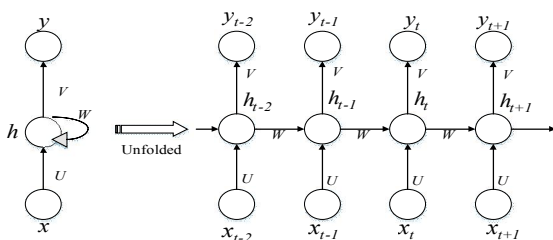


Figure 1. RNN unfolded (left), and RNN folded (right)

where g is the activation function such as *sigmoid*, *tanh*, or *ReLU*. The staple technique for training feedforward neural networks is to find backpropagation error and update the network weights. Backpropagation breaks down in a recurrent neural network, because of the recurrent or loop connections. This was addressed with a modification of the Back Propagation technique called Backpropagation Through Time or BPTT.

2.2. Long Short-Term Memory Networks (LSTM)

The structure of an LSTM cell is shown in Figure 2. In this figure, at each time t , i_t , f_t , o_t and \tilde{a}_t are input gate, forget gate, output gate and candidate value [9], which can be described as following equations:

$$i_t = \sigma(W_{i,x}x_t + W_{i,h}h_{t-1} + b_i) \quad (3)$$

$$f_t = \sigma(W_{f,x}x_t + W_{f,h}h_{t-1} + b_f) \quad (4)$$

$$o_t = \sigma(W_{o,x}x_t + W_{o,h}h_{t-1} + b_o) \quad (5)$$

$$\tilde{a}_t = \tanh(W_{\tilde{a},x}x_t + W_{\tilde{a},h}h_{t-1} + b_{\tilde{a}}) \quad (6)$$

where $W_{i,x}$, $W_{i,h}$, $W_{f,x}$, $W_{f,h}$, $W_{o,x}$, $W_{o,h}$, $W_{\tilde{a},x}$ and $W_{\tilde{a},h}$ are weight matrices, b_i , b_f , b_o and $b_{\tilde{a}}$ are bias vectors, x_t is the current input, h_{t-1} is the output of the LSTM at the previous time $t - 1$, and $\sigma()$ is the *Sigmoid* activation function. The forget gate determines how much of prior memory value should be removed from the cell state. Similarly, the input gate specifies new input to the cell state. Then, the cell state a_t is computed as:

$$a_t = f_t \circ a_{t-1} + i_t \circ \tilde{a}_t \quad (7)$$

where \circ denotes the Hadamard product. The output h_t of the LSTM at the time t is derived as:

$$h_t = o_t \circ \tanh(a_t) \quad (8)$$

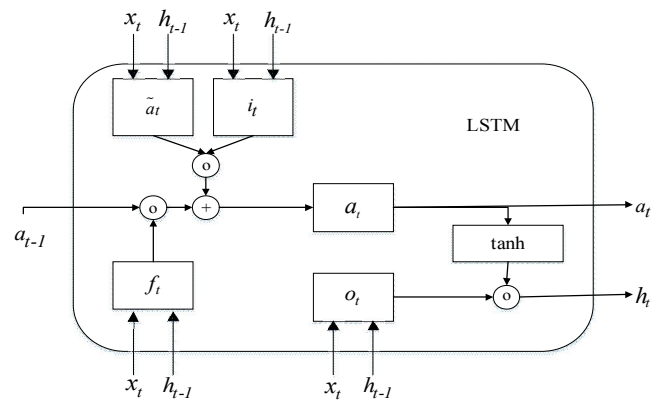


Figure 2. Structure of an LSTM cell

Finally, we project the output h_t to the predicted output \hat{z}_t as:

$$\hat{z}_t = W_y h_t \quad (9)$$

where W_y is a projection matrix to reduce the dimension of h_t . Figure 3 shows a structure of the LSTM networks unfolded in time. In this structure, an input feature vector x_t is fed into the networks at the time t . The

LSTM cell at current state receives a feedback h_{t-1} from the previous LSTM cell to capture the time dependencies. The network training aims at minimizing the usual squared error objection function f based on targets y_t as

$$f = \sum_t \|y_t - \hat{z}_t\|^2 \quad (10)$$

by utilizing backpropagation with gradient descent. During training, the weights and biases are adjusted by using their gradients. When one batch of the training dataset fed into the network has been learned by using the backpropagation optimization algorithm, one epoch is completed. Since LSTM networks training is an offline task, the computation time for training is not critical for the application. However, prediction using the learned LSTM networks is very fast.

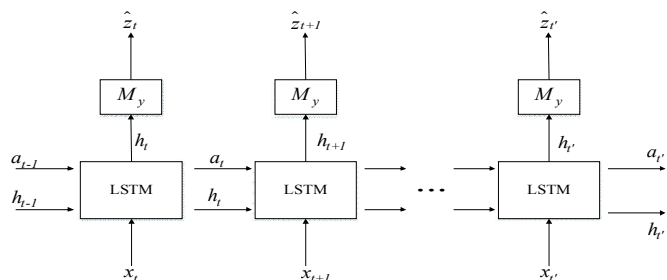


Figure 3. Structure of LSTM networks

3. RESULTS AND DISCUSSION

3.1. Solar irradiance forecasting utilizing Recurrent Neural Network

The goal here is to predict the multiple look ahead time interval values for the different setup conditions using the previous irradiance values. Although this is a huge drawback, it is also a new research-oriented that we need to improve. If we have more previous data like weather parameters, we will get more exact values. The multiple look ahead time steps are considered in such a way that predictions are made from the range of 1-h ahead values to 5-h ahead values. In such a setup, very short term predictions can be made which are useful for PV, storage control and electricity market clearing. Also, short term predictions are covered which are useful for economic dispatch and unit commitment in the context of the electricity market and power system operation [10].

The RNN was trained using online version BPTT with the modification that the network took into account both the past mistakes and the current direction to which it is moving while calculating weight updates [13].

The dataset used here is available at [18]. The solar energy resource data is available for 12 sites and out of these 12 sites, Elizabeth City State University, Elizabeth City, North Carolina is selected. The unit for the solar irradiance measured is Watts per square meter (W/m^2). Global Horizontal Irradiance (GHI) is selected for estimating solar energy. The data points are available at an interval of 5 minutes, and these data points are averaged over to get

data values at an interval of 15 minutes, 30 minutes and 1 hour. The data points are analyzed only from 8 AM to 4 PM for the period of January 2001 to December 2002.

Besides, two baseline models are selected for evaluating the performance of the proposed network. The performance indices are computed for all the three baseline models. After that, the performance of the proposed network is compared with them in each case.

- B1 is the baseline model given by the normal implementation of the BPTT network. This is the model initially formulated for the problem but it was observed that there is scope for improvement and so it was taken as the baseline model [11].

- B2 represents the persistence model. This is a naive predictor which is useful as a benchmark model in meteorology-related forecasting [12]. This model states that the future value for the next desired time instance will be the same as the latest measured value. Suppose that the time interval for which predictions are made is η and the prediction is being made for some variable p , then this model states that:

$$p_{\tau+\eta} = p_\tau \quad (11)$$

- P is the proposed model mentioned above [13]. B1 and B2 represent the two benchmark models defined earlier. Percent improvement indicates the improvement in performance of proposed model over the benchmark models.

a) 15 min instance

23360 data points were generated for this instance by taking the average of the values from provided in [18]. The number of hidden units was 25 in this case and predictions were made for $\tau+1$ and $\tau+2$ case. The results are indicated for these two cases. The proposed model was able to perform well as compared to other benchmark models for look ahead predictions of time interval greater than 2 but due to space constraint, the performance indices for these two cases is tabulated.

Table 1. Comparison of RMSE and MAE in $\tau+1$ case

Model	MAE (W/m^2)	% Improvement MAE	RMSE (W/m^2)	% Improvement RMSE
P	50.15	-	79.34	-
B1	52.36	4.4	78.35	-1
B2	49.95	-0.4	79.44	1

Table 2. Comparison of RMSE and MAE in $\tau+2$ case

Model	MAE (W/m^2)	% Improvement MAE	RMSE (W/m^2)	% Improvement RMSE
P	73.8	-	107.26	-
B1	77.42	4.9	105.46	-1.7
B2	73.94	0.2	107.86	0.6

Table 1 and Table 2 shown that the proposed model outperformed by improving 4.4% of MAE prior the normal

BPTT model but the improvement indices prior the persistence model is -0.7% for $\tau+2$ case. This might be explained that B1 model used the previous value therefore the accuracy of B1 model is better. In other case, the improvement indices are 4.9% and 0.2%. These indices indicated that the persistence model is less exact with smaller look ahead time predictions. This problem is completely logical.

b) 30 min instance

11680 data points were generated for this instance by taking the average of the values provided in [18]. The number of hidden units was 50 in this case and predictions were made for $\tau+1$ and $\tau+2$ case. The results are tabulated in two cases. The proposed model was able to perform well as compared to other benchmark models for look ahead predictions of interval greater than 2 but due to space constraint, the performance indices for these two cases is tabulated.

Table 3. Comparison of RMSE and MAE in $\tau+1$ case

Model	MAE (W/m ²)	% Improvement MAE	RMSE (W/m ²)	% Improvement RMSE
P	65.19	-	92	-
B1	70.2	7.69	93.32	1.43
B2	65.25	0.09	92.18	0.2

Table 4. Comparison of RMSE and MAE in $\tau+2$ case

Model	MAE (W/m ²)	% Improvement MAE	RMSE (W/m ²)	% Improvement RMSE
P	103.56	-	136.42	-
B1	112.39	8.5	139.32	2.1
B2	104.43	0.8	137.63	0.8

Table 3 and Table 4 shown that the proposed model outperformed by improving 7.69% of MAE prior the normal RNN but the improvement indices prior the persistence model is only 0.09% for $\tau+1$ case. In other case, the improvement indices are 8.5% and 0.8%. With 30 min interval of dataset, the proposed model gets more accurate values than 15 min case. Thus, the dependence on time interval is of great importance to predict 1h-ahead and 2h-ahead. This problem is illustrated explicitly at the next subsection.

c) 1-hour instance

5840 data points were generated for this case by taking the average of the values provided in [18]. The number of hidden units was 100 in this case and predictions were made for $\tau+1$ and $\tau+2$ cases. The results are tabulated in two cases. The proposed model was able to perform well as compared to other benchmark models in multiple look ahead predictions but due to space constraint, the performance indices for these two cases is tabulated.

In 30 min instance, the improvement indices have increased but in 1-hour instance (Table 5 and Table 6), these indices have decreased. The results of proposed model have lowest accuracy compared to the two benchmark model in

term of RMSE. However, the proposed model outperformed with the improvement on B1 model is 4.93%.

Table 5. Comparison of RMSE and MAE in $\tau+1$ case

Model	MAE (W/m ²)	% Improvement MAE	RMSE (W/m ²)	% Improvement RMSE
P	99.88	-	127.36	-
B1	99.26	-0.06	123.39	-3.22
B2	93.91	-6.4	121.79	-4.37

Table 6. Comparison of RMSE and MAE in $\tau+2$ case

Model	MAE (W/m ²)	% Improvement MAE	RMSE (W/m ²)	% Improvement RMSE
P	154.30	-	208.26	-
B1	161.91	4.93	196.3	-6.1
B2	155.9	1.6	193.6	-7.57

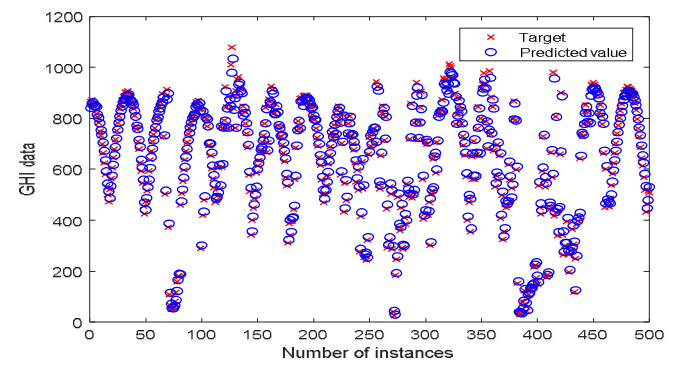


Figure 4. Output for 15 min case with $\tau+1$ prediction given by proposed method

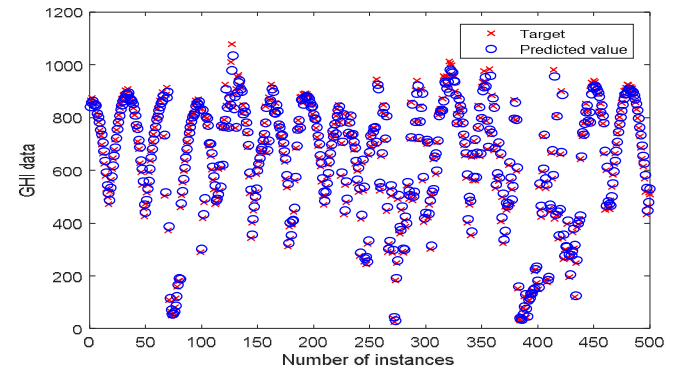


Figure 5. Output for 15 min case with $\tau+2$ prediction given by proposed method

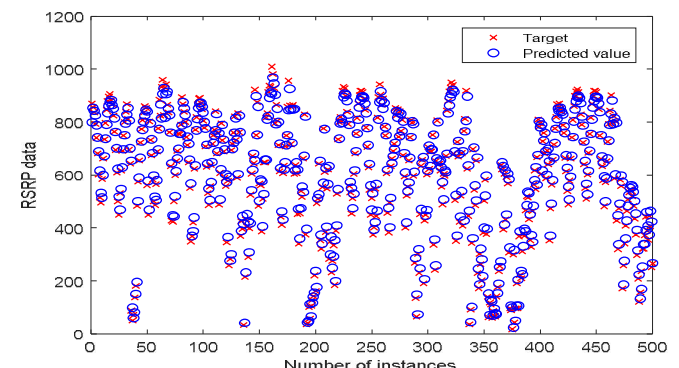
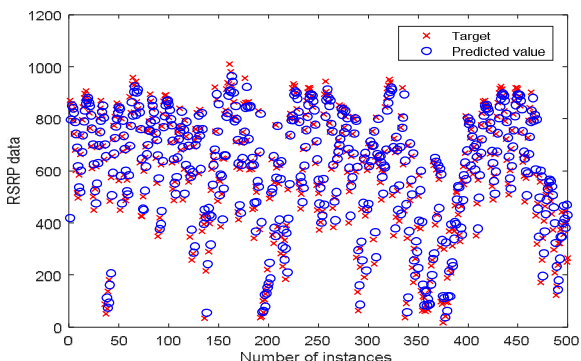
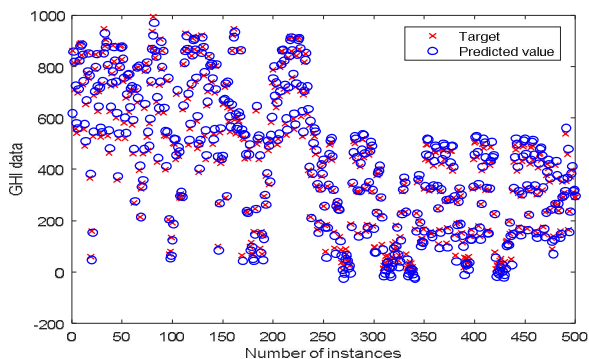
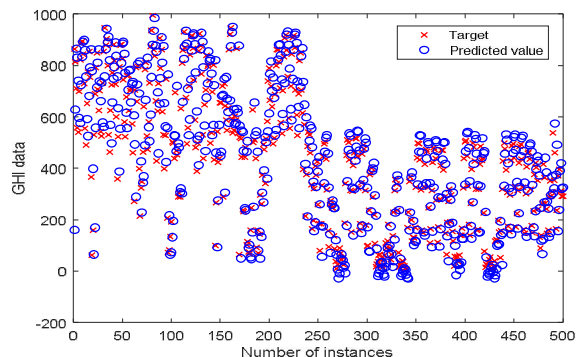


Figure 6. Output for 30 min case with $\tau+1$ prediction given by proposed method

Figure 7. Output for 30 min case with $\tau+2$ prediction given by proposed methodFigure 8. Output for 1-hour case with $\tau+1$ prediction given by proposed methodFigure 9. Output for 1-hour case with $\tau+2$ prediction given by proposed method

The multiple look ahead time predictions are done with just predicting increasing the time interval for the output without using any iterative approach to use the output as input $n-1$ times to get $\tau+\eta$ prediction. But as observed in the prediction of $\tau+2$ case with 1-hour interval data (in figure 9), the results were obtained with a slight shift towards left which indicates that the gradient is vanishing. This problem is usually seen in BPTT and it is mentioned in next section.

3.2. Solar irradiance forecasting utilizing LSTM

The gradient of RNNs can be difficult to tract in long-term memorization when they use their connection for short-term memory. Therefore, the gradient might either vanish or explode [14]. The long-term, short-term memory (LSTM) method was introduced to overcome vanishing or exploding gradient. An experiment on a dataset covering 11 years hourly data from the Measurement and

Instrumentation Data Center (MIDC) [16] by using the Keras deep learning package [17] was performed. Irradiance and Meteorological data from NREL (National Renewable Energy Laboratory) solar radiation research laboratory (BMS) station were used in the experiment, which can be publicly obtained. Average hourly dew point temperature (Tower), relative humidity (Tower), cloud cover (Total), cloud cover (opaque), wind speed (220) and east sea-level pressure were selected as weather variables. Maximum epochs were set to be 100 for LSTM. The optimal hidden neurons for LSTM from 30 to 85 with step size 5 by minimizing the RMSE of predicted irradiance values on the validation dataset were searched. Consequently, hidden neurons were set to be 30. We compared the prediction performance of the proposed LSTM networks algorithm with that of two benchmarking algorithms: the persistence method and the ANN using the classical backpropagation algorithm (BPNN). These algorithms and their parameters setting are described as follows:

- The persistence algorithm simply sets the hourly irradiance value $\tilde{y}_{d-1,t}$ at hour t in the previous day $d-1$ to be the day-ahead prediction value $\tilde{y}_{d,t}$ in the day d . Thus, this algorithm is free of training procedure and parameters setting. The persistence algorithm is frequently used as a baseline algorithm.

- The used BPNN consists of one input layer, one hidden layer and one output layer. The hidden layer neurons were set to be 50 after we made a number of experiments for an optimal choice of the hidden layer neurons. The hourly feature vectors of the training dataset were fed into the input layer, while the output layer provided the predicted hourly solar irradiance values. The sigmoid function was used for all three layers. The 'traingd' (gradient descent) was selected as the training algorithm. Performance was measured by minimizing mean square error. Maximum epochs were set to be 2500. Similarly, the used BPNN in the experiment consists of two hidden layers with 25 and 15 neurons, respectively.

Table 7 summarizes the results. With RMSE comparisons, the LSTM algorithm has significantly smaller RMSE value compared to all other algorithms. The prediction RMSE using LSTM decreases by 47% against BPNN and 63.67% against the Persistence model [15]. The performance improvement should be partially attributed to the large-scale training dataset and two important meteorological parameters about cloud cover. Generally speaking, the larger is the training dataset for LSTM, the more accurate the prediction is.

Table 7. Experimental results on the MIDC dataset

Algorithm	Testing RMSE (W/m^2)
Persistence	207.35
BPNN	142.12
LSTM	75.32

(Source: [15])

Table 8. LSTM forecasting architecture based on Keras

```

model = Sequential()
model.add(LSTM(200, batch_input_shape=(batch_size, lag, 3),
return_sequences = True))
model.add(Dropout(0.25))
model.add(LSTM(200, batch_input_shape=(batch_size, lag, 3),
return_sequences = True))
model.add(Dropout(0.25))
model.add(LSTM(30, batch_input_shape=(batch_size, lag, 3)))
model.add(Dense(1))
model.compile(loss="mean_squared_error", optimizer = 'adam')
model.fit(X_train, y_train, epochs = 100, batch_size = 219, verbose
= 2, shuffle=False)

```

4. CONCLUSION

In this paper, the deep learning algorithm BPTT was implemented for the RNN and an LSTM networks based algorithm for predicting hourly day-ahead solar irradiance has been presented. Using BPTT online version as the training approach in RNN improves about 1 - 5% in MAE and RMSE against other methods, such as Persistence Model and RNN used the normal BPTT. However, the training time for the case of t+1 with 15 min time interval is about 30 seconds on a CPU with an intel i5 processor and computed using MATLAB. This problem is perhaps a strongpoint of the methods then we can improve to get more accurate values thanks to this proposed model. +A lag was observed when the look ahead predictions were done for a time interval of greater than 5.

LSTM is a kind of recurrent neural network that perhaps prevents vanishing gradients. For the MIDC dataset with 9 years training data and 1-year validation data, the proposed LSTM algorithm is able to show a relative improvement of 47% on 1-year testing data as compared to BPNN in terms of the RMSE.

Because implementation two discussed methods on the same dataset is not completed, so in this paper we do not have a RMSE comparison between two proposed models. However, the results are expected that LSTM has better performance than RNN. Future work will focus on evaluating the accuracy in the predicted solar irradiance of two proposed methods on the same dataset. Compared to the PV output data, the historical data of irradiance is usually available. This fact makes the PV output forecast is more feasible since the direct PV output forecast requires measured data. However, obtaining this data might be impossible in new PV power plants.

REFERENCES

- [1]. Huang CMT, Huang YC, Huang KY, 2014. *A hybrid method for one-day ahead hourly forecasting of PV power output*. Proc 2014 9th IEEE Conf Ind Electron Appl ICIEA 2014. 2014;5(3):526–31.
- [2]. Yang D, Gu C, Dong Z, Jirutitjaroen P, Chen N, Walsh WM, 2013. *Solar irradiance forecasting using spatial-temporal covariance structures and time-*

forward kriging. Renew Energy [Internet]. 2013;60:235–45. Available from: <http://dx.doi.org/10.1016/j.renene.2013.05.030>

[3]. Wang Z, Wang F, Su S, 2011. *Solar irradiance short-term prediction model based on BP neural network*. Energy Procedia. 2011;12:488–94.

[4]. Mellit A, Pavan AM, 2010. *A 24-h forecast of solar irradiance using artificial neural network: Application for performance prediction of a grid-connected PV plant at Trieste, Italy*. Sol Energy [Internet]. 2010; 84(5):807–21. Available from: <http://dx.doi.org/10.1016/j.solener.2010.02.006>

[5]. Shaddel M, Javan DS, Baghernia P, 2016. *Estimation of hourly global solar irradiation on tilted absorbers from horizontal one using Artificial Neural Network for case study of Mashhad*. Renew Sustain Energy Rev [Internet]. 2016;53:59–67. Available from: <http://dx.doi.org/10.1016/j.rser.2015.08.023>

[6]. Moghaddamnia A, Remesan R, Kashani MH, Mohammadi M, Han D, Piri J, 2009. *Comparison of LLR, MLP, Elman, NNARX and ANFIS Models-with a case study in solar radiation estimation*. J Atmos Solar-Terrestrial Phys [Internet]. 2009;71(8–9):975–82. Available from: <http://dx.doi.org/10.1016/j.jastp.2009.04.009>

[7]. Alzahrani A, Shamsi P, Dagli C, Ferdowsi M, 2017. *Solar Irradiance Forecasting Using Deep Neural Networks*. Procedia Comput Sci [Internet]. 2017;114:304–13. Available from: <https://doi.org/10.1016/j.procs.2017.09.045>

[8]. Lecun Y, Bengio Y, Hinton G, 2015. *Deep learning*. Nature. 2015;521(7553):436–44.

[9]. Fischer T, Krauss C, 2018. *Deep learning with long short-term memory networks for financial market predictions*. Eur J Oper Res [Internet]. 2018;270(2):654–69. Available from: <https://doi.org/10.1016/j.ejor.2017.11.054>

[10]. Wan C, Zhao J, Song Y, Xu Z, Lin J, Hu Z, 2016. *Photovoltaic and solar power forecasting for smart grid energy management*. CSEE J Power Energy Syst. 2016;1(4):38–46.

[11]. Sfetsos A, Coonick AH, 2000. *Univariate and multivariate forecasting of hourly solar radiation with artificial intelligence techniques*. Sol Energy. 2000;68(2):169–78.

[12]. Campbell SD, Diebold FX, 2005. *Weather forecasting for weather derivatives*. J Am Stat Assoc. 2005;100(469):6–16.

[13]. Sharma AA, 2017. *Univariate short term forecasting of solar irradiance using modified online backpropagation through time*. 20th Int Comput Sci Eng Conf Smart Ubiquitous Comput Knowledge, ICSEC 2016. 2017;

[14]. Pascanu R, Gulcehre C, Cho K, Bengio Y, 2014. *How to construct deep recurrent neural networks*. 2nd Int Conf Learn Represent ICLR 2014 - Conf Track Proc. 2014;1–10.

[15]. Qing X, Niu Y, 2018. *Hourly day-ahead solar irradiance prediction using weather forecasts by LSTM*. Energy [Internet]. 2018;148:461–8. Available from: <https://doi.org/10.1016/j.energy.2018.01.177>

[16]. midcdmz.nrel.gov Access on Dec 12, 2019

[17]. https://keras.io/. Access on Oct 8, 2019

[18]. Cooperative Networks for Renewable Resource Measurements (CONFRRM) solar energy resource data. Available: http://rredc.nrel.gov/solar/new_data/confrm/ Access on Dec 12, 2019.

THÔNG TIN TÁC GIẢ

Nguyễn Đức Tuyên¹, Vũ Xuân Sơn Hữu¹, Nguyễn Quang Thuấn²

¹Viện Điện, Trường Đại học Bách khoa Hà Nội

²Trường Đại học Công nghiệp Hà Nội